Journal of Alloys and Compounds 503 (2010) 468–473

Contents lists available at ScienceDirect

Journal of Alloys and Compounds

journal homepage: www.elsevier.com/locate/jallcom

Investigation of physical properties of quaternary $AgGa_{0.5}In_{0.5}Te_2$ thin films deposited by thermal evaporation

H. Karaagac, M. Parlak*

Department of Physics, Middle East Technical University, 06531 Ankara, Turkey

ARTICLE INFO

Article history:
Received 12 November 2009
Received in revised form 7 May 2010
Accepted 13 May 2010
Available online 20 May 2010

PACS:
61.05.cp, 72.40.+w, 81.10.Fq, 81.15.−z, 88.40.H−

Keywords:
X-ray diffraction
Photoconduction
Crystal growth
Vacuum deposition
Solar cells

ABSTRACT

The aim of this study is to understand the structural, optical and photo-electrical properties of the quaternary chalcogenide $AgGa_{0.5}In_{0.5}Te_2$ thin films deposited onto the glass substrates by thermal evaporation of the single crystalline powder. Energy dispersive X-ray analysis (EDXA) showed remarkable change in atomic percentage of the constituent elements after annealing. The X-ray diffraction (XRD) of the films below the annealing temperature of 300 °C indicated the polycrystalline structure with co-existence of $AgGaTe_2$ and $AgGa_{0.5}In_{0.5}Te_2$ phases. However, the single phase of $AgGa_{0.5}In_{0.5}Te_2$ chalcopyrite structure was obtained at the annealing of 300 °C. The band gap values were calculated in between 1.05 and 1.37 eV depending on annealing temperature. The temperature dependent photoconductivity was measured under different illumination intensity. The nature of existing trap levels were studied by measuring the variation of photocurrent as a function of illumination intensity. The analysis showed that $AgGa_{0.5}In_{0.5}Te_2$ thin film changes its behavior from the sublinear to supralinear photoconductivity after annealing.

1. Introduction

In recent years, polycrystalline I–III–VI_2 chalcopyrite compound thin films, especially $CuInSe_2$ (CIS) and their quaternary counterparts such as, Cu(In,Ga)Se_2 (CIGS) and Ag(In,Ga)Se_2 are taking considerable attention of the researchers. The chalcopyrite structure has ternary analogue of II–VI zincblende structure that can be constructed by doubling the sublattice in vertical direction. In the chalcopyrite structure, tetragonal distortion and compression can be defined as a measure of the anions (VI) displacement and uniaxial distortion of the lattice cell ($c/a \neq 2$) [1]. Their fascinating optical and electrical properties, especially, allowing to tune the band gap values of these compounds by the formation of various solid solutions and having high absorption coefficients, makes them an efficient absorber in the fabrication of thin film solar cells [1–3]. It is also well known that these types of semiconductors are the potential materials for the nonlinear optical applications like narrow-band filters [4–6] and, up- and down-conversion of frequencies for the near- and mid-IR spectral region [1,7,8]. Furthermore, the direct band gap energy and flexibility in values (ranging from 3.5 eV for $CuAlS_2$ to 1.0 eV for $CuInSe_2$) make the thin film chalcopyrite materials as promising candidates for light emitting devices [1,9]. However, we have not encountered any study on polycrystalline quaternary Ag(In,Ga)Te_2 thin films except reported on solid solution of $AgGa_xIn_{1-x}Te_2$ [10]. A few studies were reported for $AgInTe_2$ and $AgGaTe_2$ thin films grown by different deposition techniques [11–14]. These are taking the attention because of their potential applications for second harmonic generation, optical parameter oscillation [15], heterojunction solar cells and infrared light sources [16,17]. In the present study, an attempt was made to investigate the structural, optical and photo-electrical properties of quaternary $AgGa_{0.5}In_{0.5}Te_2$ thin films deposited by thermal evaporation method and the results presented in this study are the typical results obtained from the five sets of the samples deposited under the same conditions.

2. Experimental details

The synthesis of $AgGa_{0.5}In_{0.5}Te_2$ was carried out by the direct reaction of stoichiometric quantities of highly pure elements of Ag, Ga, In and Te in a chemically cleaned quartz crucible sealed in a pressure of 10^{-4} Pa. It was 14 mm in diameter and 150 mm in length with a tapered bottom to improve the nucleation during the crystallization. The crucible was kept at horizontal furnace in temperature of 1050 °C for 96 h. Following to the sintering process, the single crystal of $AgGa_{0.5}In_{0.5}Te_2$ was obtained by placing crucible in a Crystalox MSD-4000 model three zone vertical Bridgman–Stockbarger system with a special gradient and temperature profile. Temperatures of upper (high), middle (medium) and bottom (low) zones were raised to 1050, 900 and 700 °C, respectively, and the crucible was maintained in the high temperature zone for 24 h for ensuring homogeneity of $AgGa_{0.5}In_{0.5}Te_2$. Temperature gradient and pulling rate were 13 K/cm and 1 mm/h, respectively. Following to a 130 h translation from the top to bottom zone and subsequent cooling down

* Corresponding author. Tel.: +90 312 2107646; fax: +90 312 2105099.
E-mail address: parlak@metu.edu.tr (M. Parlak).

0925-8388/$ – see front matter © 2010 Elsevier B.V. All rights reserved.
doi:10.1016/j.jallcom.2010.05.035

of the furnace to the room temperature, the single crystal $AgGa_{0.5}In_{0.5}Te_2$ was produced. After the growth, ingot was extracted carefully from the ampoule. The ingot was free of crack with a 13 mm in diameter and 30 mm in length. EDXA and XRD measurements carried out on the pieces taken from the different part of the ingot revealed a high crystallinity and good stoichiometry as compared with the starting material and crystal data. The powder obtained from the single crystalline ingot was used as the evaporation source and the deposition process was done onto the soda–lime glass substrates which were kept at constant temperature of 150 °C under the vacuum with the base pressure of about 10^{-4} Pa by using thermal evaporation method. During the deposition, the thickness and deposition rate of films were monitored simultaneously with a quartz crystal monitor (Inficon XTM/2). Following to the deposition, thicknesses of the films were also measured electromechanically by a Dektak 6 M profilometer and found to be around 500 nm. The annealing process was carried out in the temperature range of 250–400 °C under the constant nitrogen flow in a specially designed furnace for 30 min. The compositions of the powder and deposited $AgGa_{0.5}In_{0.5}Te_2$ thin films were defined by using a FEI Quanta 400 FEG model scanning electron microscopy (SEM) equipped with EDAX. To determine the surface composition of the deposited films, the X-ray photoelectron spectroscopy (XPS) measurements were carried out by using a UNISPECS ESCA system equipped with a MgKα radiation source of energy value of 1253.6 eV in a high vacuum system with a base pressure of about 10^{-7} Pa. The X-ray diffraction patterns of samples were obtained by using a Rigaku Miniflex XRD system equipped with CuKα X-ray source. The optical transmission and reflection measurements were carried out by using Shimadzu UV-1201 UV–VIS–NIR spectrophotometer over the wavelength range of 300–1100 nm. For the photo-electrical measurements, contacts to the samples with van der Pauw geometry were made by the evaporation of the pure indium. Then, copper electrodes were attached by using silver paste and their ohmic behaviors were confirmed through the linear variation of the polarity independent applied current. The temperature dependent photoconductivity measurements in the temperature range of 100–460 K were carried out under the vacuum of about 1.3×10^{-2} Pa in a Janis liquid nitrogen cryostat equipped with a Lake Shore 331 temperature controller. The samples were illuminated perpendicularly by a halogen lamp during the photoconductivity measurements under different illumination intensities varying in between 20 to 115 mW/cm^2.

3. Results and discussions

3.1. Compositional analysis

The compositions of evaporation source powder, as-grown and $AgGa_{0.5}In_{0.5}Te_2$ thin films annealed at 300 and 400 °C were determined by EDAX measurements conducted at the acceleration voltage of 10 kV. The results obtained for the powder and the annealed films are given in Table 1.

It was observed that the compositions of source powder were nearly stoichiometric within the experimental error limit, while it was not the case for the as-grown and annealed samples. Since the as-grown $AgGa_{0.5}In_{0.5}Te_2$ thin films have Te-rich and Ag-, Ga-, and In-deficient composition. Furthermore, there is a remarkable change in atomic percentage of constituent elements with the annealing, such as, the atomic percentage of Te is decreasing considerably after the annealing. The existence of excess Te in the as-deposited samples can be attributed to the different vapor pressures of constituent elements ranked as $P_{Te} > P_{In} > P_{Ag} > P_{Ga}$. Therefore, it is reasonable to expect that Te and In elements play an important role in the evaporation process and dominate the composition of the grown films. The decrease in atomic percentage of Te is probably related with the re-evaporation of high volatile nature of these atoms just before constructing bonds with other ad-atoms during the crystallization observed following to the annealing [18].

Table 1
EDAX results for the source powder, as-grown and annealed $AgGa_{0.5}In_{0.5}Te_2$ thin films at 300 and 400 °C.

Atomic percent (at.%) ±2%				
Sample	Ag	Ga	In	Te
Starting material	25.00	12.50	12.50	50.00
Powder	23.17	13.13	13.59	50.11
As-grown	22.65	10.84	09.29	57.22
300 °C	29.75	12.17	09.44	48.64
400 °C	30.29	23.46	07.98	38.27

To compare the surface composition with the bulk and understand the effect of annealing on the morphology, the XPS measurements were carried out for the as-grown and the films annealed at different temperatures.

Fig. 1 shows the XPS spectrum of the as-grown and film annealed at 300 °C. The spectral shift due to the surface charging effect was corrected by taking carbon (C) 1s photoelectron peak at binding energy (284.6 eV) as reference value. It is clearly seen from the XPS survey spectra of both as-grown and annealed film (Fig. 1), all expected constituent elements (Ag, Ga, In, and Te) are appeared on the surface composition with corresponding photoelectron lines. In addition, apart from the constituent elements, the C 1s and oxygen (O) 1s peaks are identified in the spectrum. The presence of C and O is likely to be due to the contamination of the samples during the exposure to atmosphere and measurement stages. The existence of remarkable O is probably originating from the formation of an oxide layer on the surface. To reduce the amount of these contaminations, the samples were sputtered by argon (Ar) ions accelerated with energy of 2000 eV for 5 and 8 min. The variation in survey spectrum following to the sputtering process is shown in Fig. 1 for both as-grown and annealed films. It can be seen that the concentration of C and O reduces substantially after sputtering. Especially, a considerable decrease in relative intensity of C 1s was observed along with increasing the sputtering time for both as-grown and annealed

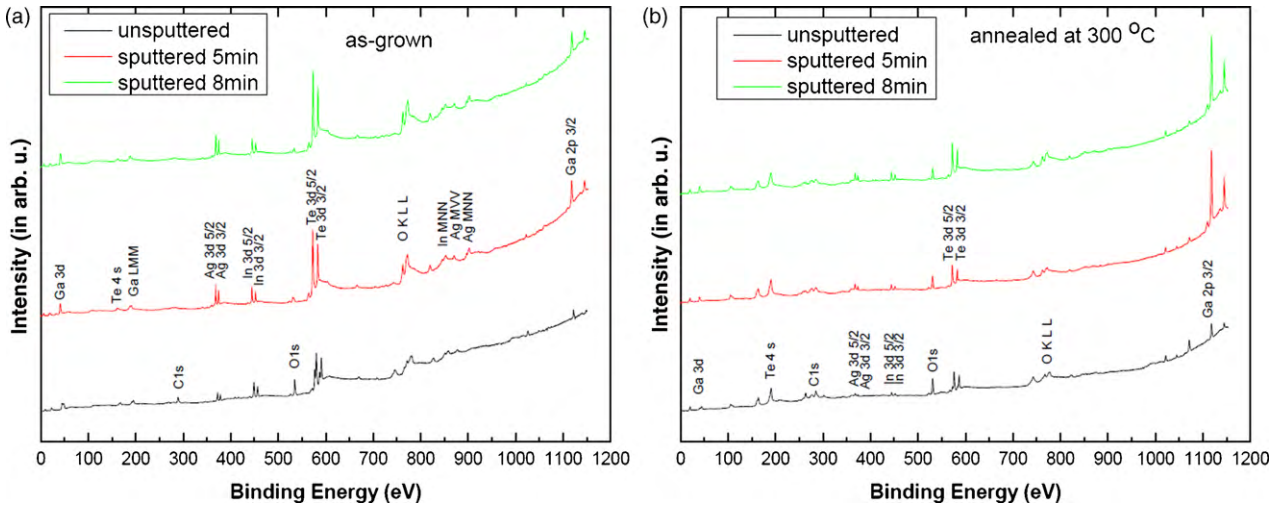

Fig. 1. XPS survey spectrum for (a) as-grown and (b) $AgGa_{0.5}In_{0.5}Te_2$ thin film annealed at 300 °C.

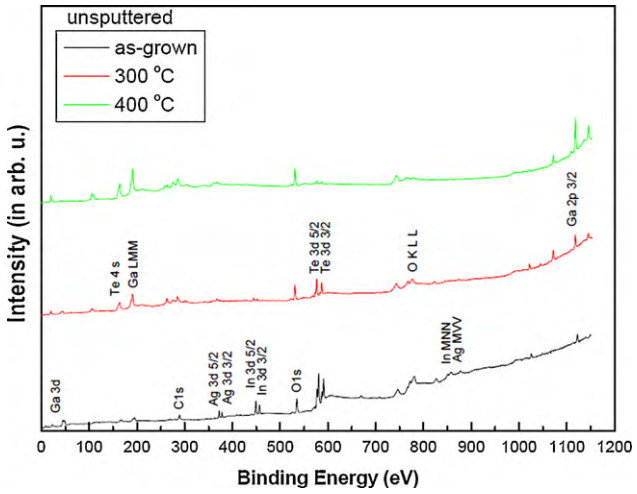

Fig. 2. XPS survey spectrum for the surface unsputtered as-grown and films annealed at 300 and 400 °C.

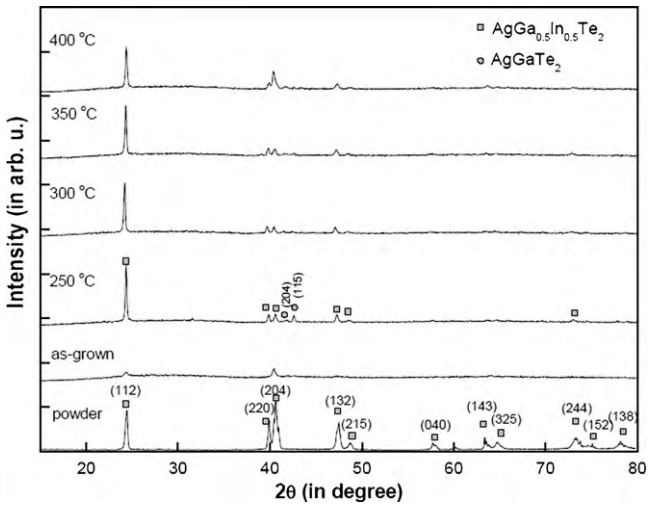

Fig. 4. X-ray diffraction pattern of powder, as-grown and $AgGa_{0.5}In_{0.5}Te_2$ thin film annealed in the temperature range of 250–400 °C.

samples, which suggests a decrease in C concentration on the surface. Fig. 2 and Fig. 3 give the XPS survey spectra for the as-grown, annealed film at 300 and 400 °C for unsputtered and sputtered surfaces for 5 min, respectively. From the Fig. 2, it is clearly seen that the amount of Te on the surface is decreasing with annealing, which implies that the re-evaporation of high volatile Te from the surface. The reduction in Te content verifies the results obtained from the EDXA study. A remarkable increase in amount of Ga and a decrease in that of Ag and In along with increasing annealing temperature were also observed. The variation in the composition after sputtering follows the same trend of modification observed for the unsputtered surface except a slight variation in the relative intensities of photoelectron lines.

3.2. Structural analysis

The XRD patterns for the source powder, as-grown and $AgGa_{0.5}In_{0.5}Te_2$ films annealed at temperatures ranging from 250 to 400 °C by a step of 50 °C were illustrated in Fig. 4. The X-ray results of source powder show good structural homogeneity of the crystalline $AgGa_{0.5}In_{0.5}Te_2$ phase without any precipitation of extra elements, binary or ternary phases.

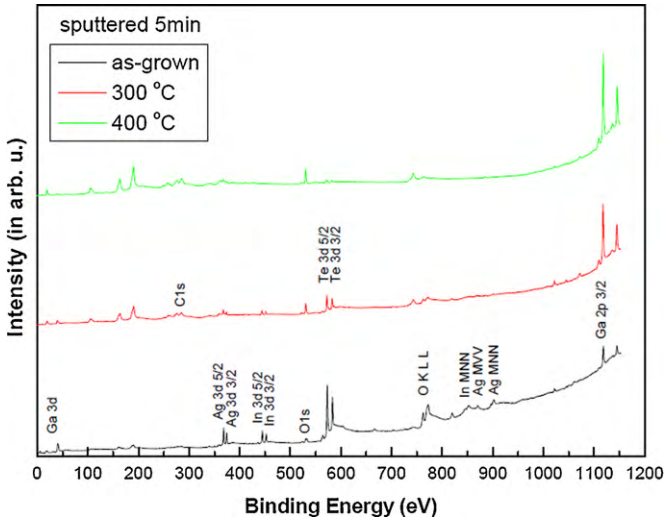

Fig. 3. XPS survey spectrum for the surface sputtered as-grown and films annealed at 300 and 400 °C.

The analysis of the powder with Checkcell software has shown a single phase of $AgGa_{0.5}In_{0.5}Te_2$ chalcopyrite structure with the lattice constants $a = b = 6.3771$ Å and $c = 12.2507$ Å and space group of *I*-42*D*. The same analysis was carried out for the deposited films and compared with those obtained for the evaporation source powder. As a result of this analysis, the unit cell parameters for the films annealed at 300 °C were obtained as $a = b = 6.3850$ Å and $c = 12.3680$ Å corresponding to $AgGa_{0.5}In_{0.5}Te_2$ with the tetragonal chalcopyrite structure. The calculated lattice parameters are in close agreement with reported values by El-Sayad [10] for the polycrystalline and the single crystalline forms of $AgGa_{0.5}In_{0.5}Te_2$. However, there is a slight difference between lattice constants obtained for the powder and the deposited films. This difference could be attributed to the segregation and/or re-evaporation of the constituent elements in the structure. As seen from Fig. 4, the as-grown $AgGa_{0.5}In_{0.5}Te_2$ film is in the polycrystalline form. Two weak peaks appeared in the diffractogram of as-grown film were identified as (1 1 2) and (2 0 4) diffractions that are the characteristic diffraction peaks of the $AgGa_{0.5}In_{0.5}Te_2$ chalcopyrite structure. On the other hand, new diffraction peaks corresponding to $AgGa_{0.5}In_{0.5}Te_2$ and $AgGaTe_2$ phases start to appear depending on the annealing temperature. The (1 1 2) diffraction line corresponding to Bragg's angle $2\theta = 24.35°$ is the strongest peak and confirming the preferred orientation direction of $AgGa_{0.5}In_{0.5}Te_2$ thin films. The lines indexed as (2 0 4) and (1 1 5) were identified to be belonging to $AgGaTe_2$ phase [19]. XRD study reveals that annealing at 250 °C leads to a remarkable improvement in $AgGa_{0.5}In_{0.5}Te_2$ phase and arising of additional $AgGaTe_2$ phase. No remarkable change was observed with further increases in the annealing temperature up to 300 °C except almost disappearance of $AgGaTe_2$ phase and small decrease in full width at half maxima (FWHM) of (1 1 2) diffraction line, which is the indication of better crystallinity. However, as seen from Fig. 4, there is a small decrease in the intensity of (1 1 2) diffraction line and increase in that of (2 0 4) following to the annealing at 400 °C. This indicates the structural modification related with the segregation and/or re-evaporation of the constituent elements at high annealing temperature.

SEM micrographs of the as-grown and the annealed films (Fig. 5) confirm the enhanced crystallinity after annealing. It is clearly seen that the surface is composed of grains with different sizes (varying from 250 nm to 1 μm) increasing with the annealing as a consequence of the given thermal energy.

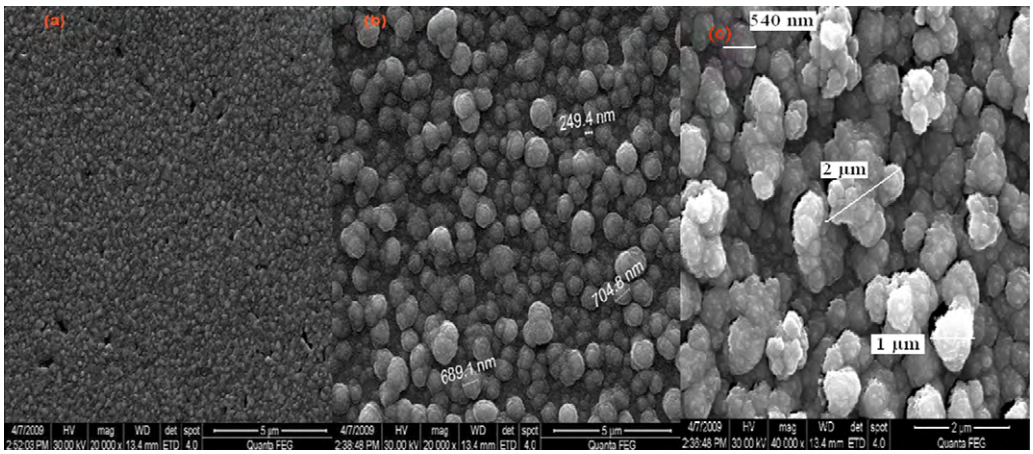

Fig. 5. The SEM micrograph for (a) as-grown and $AgGa_{0.5}In_{0.5}Te_2$ thin film annealed at (b) 300 °C and (c) 400 °C.

In order to determine the average grain size of both as-deposited and the annealed films, the Scherrer's formula was used;

$$D = \frac{0.94\lambda}{\beta \cos\theta} \quad (1)$$

where λ is the wavelength of X-ray, θ is the Bragg angle, and β is the FWHM. As a result of calculation, the average grain sizes of the as-deposited and $AgGa_{0.5}In_{0.5}Te_2$ film annealed at 250 °C were found to be around 20 and 48 nm, respectively. There was no change in the grain sizes with further annealing up to 350 °C. However, after subsequent annealing at 400 °C, they were around 36 nm. When the grain sizes obtained from both methods are compared, there is a large difference in the evaluated and the measured values. This is closely related with that the grain sizes appeared in SEM images are the grains only at the surface of films, while grain size calculated from the XRD is the average value of the grain sizes distributed throughout the thickness of the film. The same result was reported by Matsuo et al. [20].

3.3. Optical analysis

Fig. 6 shows the transmittance and reflectance spectra of the as-deposited and $AgGa_{0.5}In_{0.5}Te_2$ films annealed at 250, 300 and 400 °C measured in the wavelength range of 400–1100 nm. As seen from the figure, the reflectance decreases upon applying the annealing process.

The high reflection observed in the spectra of the as-grown film can be taken as the indication of Ag- and Te-rich film surface behaving like a metallic surface and reflecting the most of incoming light. The decrease in reflection after annealing could be attributed to the decrease in the atomic percentage of Te and Ag on the film surface as observed from EDXA and XPS studies. It is also important to note that the transmission is reduced and cut-off shifts to the shorter wavelength with the annealing that is most probably related to the changes observed in the structural modification of film surface as deduced from XRD, XPS and EDXA studies.

The band gap values were determined by means of analyzing the transmission and reflection spectra shown in Fig. 6. The absorption coefficient (α) was evaluated through the following expression [21]:

$$T = (1 - R)^2 \exp(-\alpha t) \quad (2)$$

where T is transmittance, R is reflectance and t is the thickness of the sample.

For the allowed direct band gap transition, α is related to photon energy ($h\nu$) through the following expression [22]:

$$(\alpha h\nu)^2 = A(h\nu - E_g) \quad (3)$$

where A is a constant and E_g is the optical band gap energy. The plot of $(\alpha h\nu)^2$ against ($h\nu$) for the as-grown and annealed $AgGa_{0.5}In_{0.5}Te_2$ film at 250, 300 and 400 °C is shown in Fig. 7.

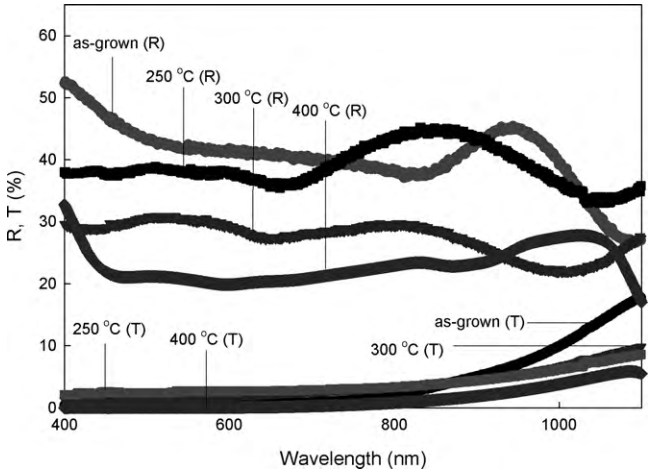

Fig. 6. Transmission and reflection spectrum of as-grown and $AgGa_{0.5}In_{0.5}Te_2$ film annealed at 250, 300 and 400 °C.

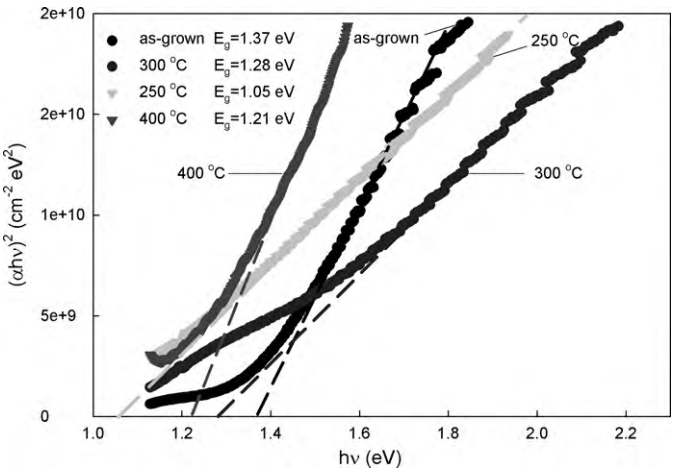

Fig. 7. Plot of $(\alpha h\nu)^2$ against ($h\nu$) for as-grown and $AgGa_{0.5}In_{0.5}Te_2$ film annealed at 250, 300 and 400 °C.

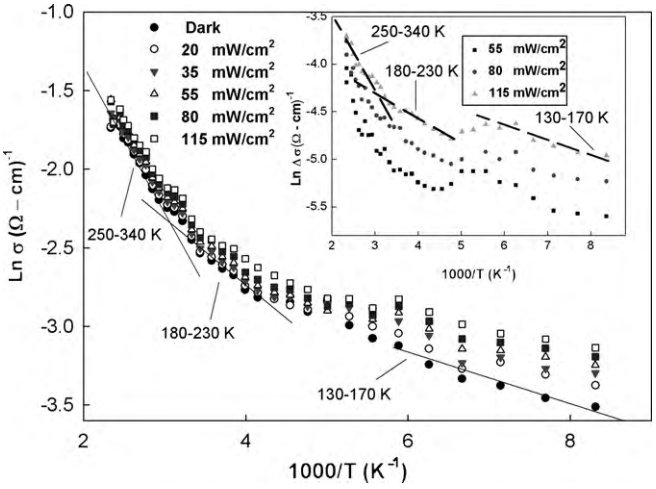

Fig. 8. The variation of the photoconductivity with temperature and illumination intensity for as-grown $AgGa_{0.5}In_{0.5}Te_2$ thin film.

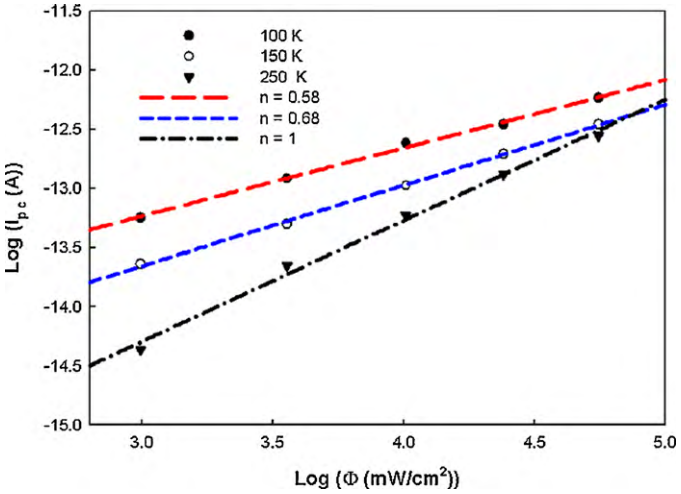

Fig. 9. The variation of photocurrent (I_{pc}) as a function of illumination intensity (Φ) at temperatures of 100, 150, and 250 K for as-grown $AgGa_{0.5}In_{0.5}Te_2$ thin film.

The optical band gap values are determined by the extrapolation of the linear part of $(\alpha h\nu)^2$ vs. $(h\nu)$ relation to zero and are found to be 1.37, 1.05, 1.28 and 1.21 eV for as-grown and annealed $AgGa_{0.5}In_{0.5}Te_2$ film at 250, 300 and 400 °C, respectively. These values are very close to the values given for $AgGaTe_2$ (E_g = 1.36 eV) and $AgInTe_2$ (E_g = 1.04 eV) [15,23]. It can be concluded that the annealing results in the changes in the optical band gap that is generally explained in terms of the decrease or the increase in the degree of disorder and the defect density in the structure. In our case, the variation in the band gap after annealing may be attributed to the modification in the structure because of the segregation of the constituent elements as observed from EDXA and XRD results.

3.4. Photoconductivity

Fig. 8 shows the variation of the dark conductivity and the conductivity under the illumination intensities (ϕ) of 20, 35, 55, 80 and 115 mW/cm^2 as a function of reciprocal temperature for as-grown $AgGa_{0.5}In_{0.5}Te_2$ thin film.

Photoconductivity ($\Delta\sigma$) can be expressed via the subtraction of the dark conductivity from the conductivity measured under illumination. The variation of photoconductivity under illumination intensities of 55, 80 and 115 mW/cm^2 for the as-grown $AgGa_{0.5}In_{0.5}Te_2$ thin film is shown in the inset of Fig. 8. As seen from the figure, there is an exponential variation of the conductivity in between 9×10^{-3} and 4×10^{-2} $(\Omega\,\mathrm{cm})^{-1}$ with increasing temperature and illumination intensity. Three different regions under each illumination intensity can be distinguished. From the calculated activation energies for dark conductivity and photoconductivity under the illumination intensity of 115 mW/cm^2, it was found that the values for both cases are almost the same. The activation energy values were found to be around 10, 18 and 50 meV for 130–170 K, 180–230 K and 250–340 K temperature intervals, respectively.

As observed from the figure, at high temperatures the photoconductivity approaches a saturation value for all intensities. In deed, for a material including imperfections the increase in temperature above a critical value may result in the excitation of the minority carriers trapped at levels responsible for the long majority carrier lifetimes. These favor the rate of recombination and result in a photocurrent approaching a saturation value [24].

Generally, the saturation behavior of a photocurrent is taken as the indication of the deep trap levels. In order to determine their characteristics, the variation of photocurrent (I_{pc}) as a function of illumination intensity (ϕ) was determined. The plot in Log–Log scale is shown in Fig. 9 for as-grown $AgGa_{0.5}In_{0.5}Te_2$ thin film.

The variation was determined for the absolute temperatures of 100, 150, and 250 K. It was found that this variation obeys the $I_{pc} \propto \phi^n$ relation [25]. Here, I_{pc} is the photocurrent obtained by subtracting the total current from the dark current, ϕ is the illumination intensity, and n is the power exponent, characterizing the type of the recombination mechanism. It is known that ≈0.5 and ≈1.0 values of the exponent (n) are the indication of *bimolecular* and *monomolecular* recombination mechanism, respectively [26]. On the other hand, the value of n between 0.5 and 1.0 is the indication of existing continuous distribution of traps [27]. In our case, for the as-grown $AgGa_{0.5}In_{0.5}Te_2$ thin film, the n value was found to be varying between 0.5 and 1 and taking distinct values at different temperatures. This implies the continuous distribution of the traps acting as either *bimolecular* or *monomolecular* recombination mechanism.

Fig. 10 shows the variation of conductivity as a function of temperature in the studied temperature range for the annealed $AgGa_{0.5}In_{0.5}Te_2$ thin film under the illumination intensities of 20, 35, 55, 80 and 115 mW/cm^2. The photoconductivity for the annealed film was determined as described above and its variation as a function of temperature under the illumination intensities of 55, 80 and 115 mW/cm^2 in temperature range of 100–430 K is illustrated as inset in Fig. 10.

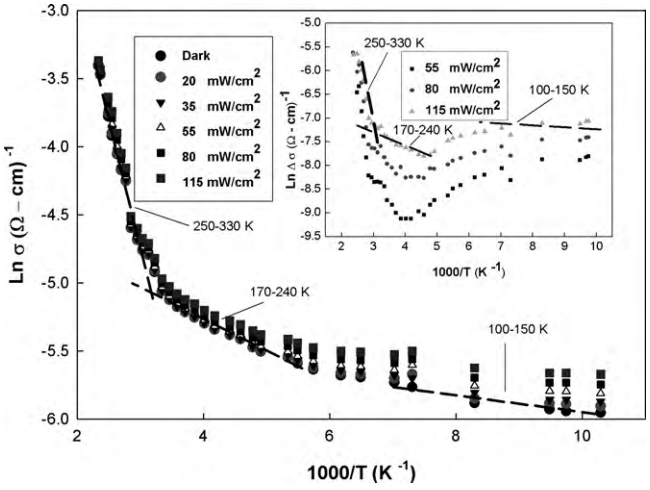

Fig. 10. The variation of the photoconductivity with temperature and illumination intensity for $AgGa_{0.5}In_{0.5}Te_2$ thin film annealed at 300 °C.

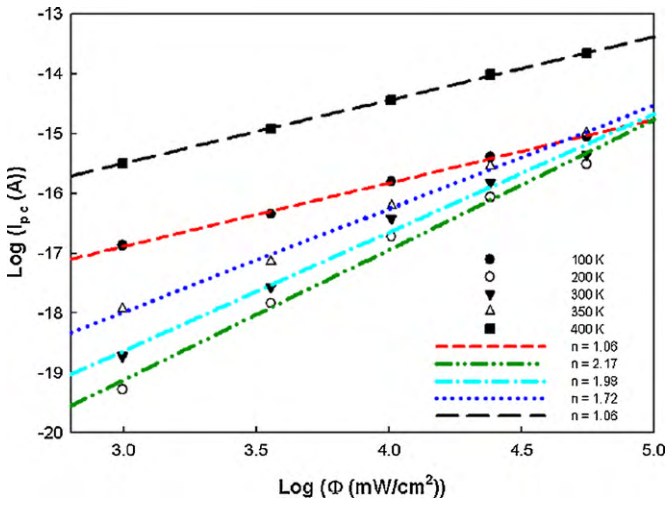

Fig. 11. The variation of the photocurrent (I_{pc}) as a function of illumination intensity (Φ) at the temperatures of 100, 200, 300, 350, 400 K for the $AgGa_{0.5}In_{0.5}Te_2$ thin film annealed at 300 °C.

The variation of the photoconductivity with temperature and illumination intensity showed a similar behavior as that of the as-grown sample. The calculated activation energy values revealed the same as those obtained from the dark conductivity measurements. They are around 6, 15, and 40 meV for 100–150 K, 170–240 K and 250–330 K temperature intervals, respectively. Slight decreased activation energies after 300 °C-annealing may be attributed to the possible modification in the grain boundary. The obtained activation energies for both as-grown and annealed samples are in close agreement with theoretically calculated values based on specific models for donors and acceptor levels in I–III–VI type compounds [28].

The existence of different activation energies is the indication of the different conduction mechanisms that are taking place at different temperature intervals. These energies for the annealed film are probably related to the defects formed by the segregation of the constituent elements within the structure and giving rise to the formation of the point defects (such as cation (Ag, Ga, In) and anion (Te) vacancies), interstitials and cation–cation antisites mostly expected in chalcopyrite I–III–VI_2 structures [28]. The deviation from stoichiometry following to the deposition and the annealing process may promote the construction of additional phases ($AgGaTe_2$) that may also be the origin of the observed trap levels. As it was done for as-grown sample, to characterize the existing recombination centers, the variation of photocurrent with the illumination intensity for the annealed $AgGa_{0.5}In_{0.5}Te_2$ thin film was measured for the constant temperature of 100, 200, 300, 350, and 400 K and is shown in Fig. 11.

From the slope of Log(I_{pc})–Log(ϕ) plot, it is deduced that the exponent of $I_{pc} \propto \phi^n$ relation is >1 for the all absolute temperatures. The situation can be explained by a two-center model which is proposing the existence of supralinear photoconductivity. That is, the lifetime of free carriers increases with the light intensity and becomes more photosensitivity [25]. As a result of the photocurrent-illumination intensity characteristics, it can be concluded that $AgGa_{0.5}In_{0.5}Te_2$ thin film changes its behavior from sublinear to supralinear photoconductivity following to the annealing process.

4. Conclusions

In this study, polycrystalline $AgGa_{0.5}In_{0.5}Te_2$ thin films with chalcopyrite structure were deposited by using the single crystalline powder produced by Bridgman–Stockbarger technique. Compositional analyses have revealed that the stoichiometry of the films changes with the annealing process. As-grown films showed Te-rich and Ag, Ga, In-deficient behaviors as compared with the stoichiometry of the starting single crystalline powder. However, annealing resulted in the decreasing in the amount of Te and In contents in the structure. In general, they play an important role in the structure of the films. These variations are also verified by means of XPS study. Depending on annealing temperature $AgGaTe_2$ and $AgGa_{0.5}In_{0.5}Te_2$ phases were observed in the XRD study, but after annealing at 300 °C single phase of tetragonal chalcopyrite structure of $AgGa_{0.5}In_{0.5}Te_2$ thin films with the preferred orientation along (1 1 2) direction were obtained.

Optical analysis showed that depending on the fluctuation in the compositions of the samples following to the annealing, the optical band gap values varied from 1.37 to 1.05 eV, which can be taken as the indication of the different energy levels in the band gap region. The analysis of the photoconductivity for all samples showed that the photocurrent values depending on the annealing temperature reached a saturation value. This behavior can be attributed to the existing of trap levels, which may be the result of the variation in constituent elements as observed from XRD and EDXA study. The study on these levels indicated that there was continuous distribution of the trap levels acting as either *bimolecular* or *monomolecular* recombination centers. At high annealing temperature, the situation in the photoconductivity changed to the supralinear behavior that can be explained by a two-center model.

Acknowledgement

This work was supported by Turkish Scientific and Research Council (TUBITAK) under Grant No. 108T019.

References

[1] J.L. Shay, J.H. Wernick, Ternary Chalcopyrite Semiconductors: Growth, Electronic Properties and Applications, Pergamon, Oxford, 1975.
[2] A. Rockett, R.W. Birkmire, J. Appl. Phys. 70 (1981) R81.
[3] H.W. Schock, Appl. Surf. Sci. 92 (1996) 606.
[4] G.D. Boyd, H.M. Kasper, J.H. McFee, F.D. Storz, IEEE J. Quantum Electron. 8 (1972) 900.
[5] N. Yamamoto, H. Takehara, H. Horinaka, T. Miyauchi, Jpn. J. Appl. Phys. 25 (1986) 1397.
[6] P.G. Schunemann, S.D. Setzler, T.M. Pollak, J. Cryst. Growth 211 (2000) 257.
[7] Y.X. Fan, R.C. Eckardt, R.L. Byer, R.K. Route, R.S. Feigelson, Appl. Phys. Lett. 45 (1984) 313.
[8] R.C. Eckardt, Y.X. Fan, R.L. Byer, R.K. Route, R.S. Feigelson, J. van der Laan, Appl. Phys. Lett. 47 (1985) 786.
[9] B.M. Başol, A. Halani, C. Laidholm, G. Norsworthy, Y.K. Kapur, A. Swatzlander, R. Matson, Prog. Photovolt. Res. Appl. 8 (2000) 227.
[10] E.A. El-Sayad, Phys. Status Solidi (a) 201 (2004) 103.
[11] S.M. Patel, B.H. Patel, Mater. Lett. 5 (1985) 35.
[12] S.M. Patel, B.H. Patel, Thin Solid Films 173 (1989) 169.
[13] R. Vaidhyanathan, S.L. Pinjare, J. Sebhanadri, Thin Solid Films 105 (1983) 157.
[14] S. Amarjit, R.K. Bedi, Thin Solid Films 398–399 (2001) 427.
[15] B. Tell, J.L. Shay, H.M. Kasper, Phys. Rev. B 9 (1974) 5203.
[16] N.N. Konstantinkova, Y.V. Rud, Sov. Phys. Semicond. 23 (1989) 1101.
[17] C. Julien, I. Ivanov, A. Khelfa, F. Alapini, M. Guittard, J. Mater. Sci. 31 (1996) 3315.
[18] A. Roth, Vacuum Technology, North-Holland, Amsterdam, 1980.
[19] JCPDS (Joint Committee on Powder Diffraction Standards) Card No:45-1278.
[20] H. Matsuo, K. Yoshino, T. Ikari, Thin Solid Films 515 (2006) 505.
[21] R. Bischel, F. Levy, Thin Solid Films 128 (1985) 75.
[22] N.F. Mott, E.A. Davis, Electronic Process in Noncrystalline Materials, Clarenden Press, Oxford, 1971.
[23] N.V. Joshi, Photoconductivity, Marcel Dekker, New York and Basel, 1990.
[24] H. Karaagac, M. Parlak, et al., Cryst. Res. Technol. 42 (2006) 1159.
[25] R.H. Bube, Photoelectronic Properties of Semiconductors, Cambridge University Press, Cambridge, 1992.
[26] R.H. Bube, Photoconductivity of Solids, Willey, New York, 1960.
[27] A. Rose, Concepts in Photoconductivity, Interscience, New York, 1960.
[28] R. Marquez, C. Rincon, Mater. Lett. 40 (1999) 66–70.